



VNS improves VSMC metabolism and arteriogenesis in infarcted hearts through m/n-AChR-Akt-SDF-1 α in adult male rats

Xing-yuan Li^{1,2} · Jia-Qi Liu³ · Yan Wang¹ · Yan Chen¹ · Wen-hui Hu¹ · Yan-xia Lv^{2,4} · Yan Wu^{2,4} · Jing Lv⁵ · Jun-ming Tang^{2,4,5} · Deying Kong¹

Received: 16 October 2022 / Accepted: 21 October 2023 / Published online: 2 January 2024
© The Author(s) 2023

Abstract

Vagal nerve stimulation (VNS) provides a novel therapeutic strategy for injured hearts by activating cholinergic anti-inflammatory pathways. However, little information is available on the metabolic pattern and arteriogenesis of VSMCs after MI. VNS has been shown to stimulate the expression of CPT1 α , CPT1 β , Glut1, Glut4 and SDF-1 α in coronary VSMCs, decreasing the number of CD68-positive macrophages while increasing CD206-positive macrophages in the infarcted hearts, leading to a decrease in TNF- α and IL-1 β accompanied by a reduced ratio of CD68- and CD206-positive cells, which were dramatically abolished by atropine and mecamylamine *in vivo*. Knockdown of SDF-1 α substantially abrogated the effect of VNS on macrophage cell alteration and inflammatory factors in infarcted hearts. Mechanistically, ACh induced SDF-1 α expression in VSMCs in a dose-dependent manner. Conversely, atropine, mecamylamine, and a PI3K/Akt inhibitor completely eliminated the effect of ACh on SDF-1 α expression. Functionally, VNS promoted arteriogenesis and improved left ventricular performance, which could be abolished by Ad-shSDF-1 α . Thus, VNS altered the VSMC metabolism pattern and arteriogenesis to repair the infarcted heart by inducing SDF-1 α expression, which was associated with the m/nAChR-Akt signaling pathway.

Keywords Myocardial infarction · Vagal nerve stimulation · Metabolism · Arteriogenesis · SDF-1 α

Abbreviations

ACh Acetylcholine
 α -SMA Alpha smooth muscle actin

Xing-yuan Li, Jia-Qi Liu and Yan Wang are co-first authors.

✉ Jing Lv
389514970@qq.com

✉ Jun-ming Tang
tangjm416@163.com

✉ Deying Kong
vsyongyer@126.com

Xing-yuan Li
836595262@qq.com

Jia-Qi Liu
1745456360@qq.com

Yan Wang
951331390@qq.com

Yan Chen
297379873@qq.com

Wen-hui Hu
hwh199707@163.com

Yan-xia Lv
350182495@qq.com

Yan Wu
2668224536@qq.com

- 1 Department of Physiology, Faculty of Basic Medical Sciences, Zunyi Medical University, Zunyi 563006, Guizhou, People's Republic of China
- 2 Hubei Key Laboratory of Embryonic Stem Cell Research, Faculty of Basic Medical Sciences, Hubei University of Medicine, Shiyan 442000, Hubei, People's Republic of China
- 3 Nursing College, Hubei Province Chinese Medicine Hospital, Hubei University of Traditional Chinese Medicine, Wuhan 430065, Hubei, People's Republic of China
- 4 Department of Physiology, Faculty of Basic Medical Sciences, Hubei University of Medicine, Shiyan 442000, Hubei, People's Republic of China
- 5 Institute of Basic Medical Sciences, Institute of Biomedicine, Hubei University of Medicine, Hubei 442000, People's Republic of China

DMEM	Dulbecco's modified Eagle's medium
LVSP	Left ventricular systolic pressure
LVEDP	Left ventricular end-diastolic pressure
+dP/dt _{max}	Rate of rise of ventricular pressure
−dP/dt _{max}	Rate of fall of ventricular pressure
M	Mol/L
SDF-1 α	Stromal cell derived factor 1 alpha

Introduction

Clinically, ischemic heart disease is often caused by vascular stenosis or obstruction caused by atherosclerotic lesions in coronary arteries, which are related to endothelial injury, proliferation and migration in vascular smooth muscle cells (VSMCs) and abnormal activation of macrophages (Li et al. 2004a). Myocardial infarction (MI), characterized by an increased ratio of sympathetic nerve to vagus nerve activity, is accompanied by an inflammatory response and macrophage infiltration, leading to myocardial injury (Lim et al. 2016). Basic and clinical studies show that vagal nerve stimulation (VNS) rebalances autonomic nerve activity in injured hearts, providing a novel therapeutic strategy for autonomic dysfunction through activating cholinergic anti-inflammatory pathways (Jones et al. 1980; Li et al. 2004a; Lim et al. 2016; Martelli et al. 2014; Shen et al. 2011). However, the anti-inflammatory roles of VNS-mediated VSMCs in infarcted hearts remain unclear.

Indeed, alterations in the differentiated state of VSMCs play a critical role in the pathogenesis of atherosclerosis and intimal hyperplasia (Chiong et al. 2013; Peiró et al. 2016; Wall et al. 2018). Increased glucose transporter 1 (Glut1) expression in VSMCs promoted VSMC phenotype switching, monocyte recruitment and atherosclerosis through increased glycolysis and the polyol pathway in vascular stenosis and metabolic disease models (Adhikari et al. 2011; Hall et al. 2001; Kaiser et al. 1993; Peiró et al. 2016; Vesely et al. 2009; Wall et al. 2018). However, little information is available on the possible relationship between VSMC metabolic patterns and angiogenesis after MI.

As a promising therapeutic target with functional performance associated with both ionotropic and metabotropic signaling, $\alpha 7$ -nicotinic ACh receptor ($\alpha 7$ -nAChR) activation can improve the progression of Parkinson's disease and Alzheimer's disease (Fontana et al. 2023), in addition to its diverse roles in cancer pathogenesis (Hajiasgharzadeh et al. 2019). Significantly, recent reports have shown that reduced levels of $\alpha 7$ -nAChR expression hamper angiogenesis in ischemic or infarcted hearts (Li et al. 2004b, 2019; Pillai et al. 2012; Yu et al. 2013). Conversely, VNS restored and even enhanced the levels of $\alpha 7$ -nAChR and m3-AChR expression in the injured heart (Zhao et al. 2013), while it increased the concentration of ACh in the ventricle of

the heart (Akiyama et al. 2001; Cooke et al. 2008; Coote et al. 2013; Kakinuma et al. 2005). Unfortunately, its potential mechanism has not been fully explored. As a classical molecule of chemokines, stromal cell-derived factor-1 α (SDF-1 α) can activate and/or induce the migration of hematopoietic/endothelial progenitor cells and endothelial cells, in addition to most leukocytes (Ceradini et al. 2004; De Falco et al. 2004; Greenbaum et al. 2013; MacArthur et al. 2013). However, whether SDF-1 α is involved in VNS-mediated anti-inflammatory and VSMC metabolism is yet to be determined.

In the present study, we found that VNS decreased the inflammatory response while increasing Glut1 expression in VSMCs of the infarcted hearts. Therefore, we hypothesized that VNS optimized VSMC metabolism patterns and inflammatory responses, resulting in improved cardiac function in infarcted hearts.

Materials and methods

Animals

In accordance with the Guide for the Care and Use of Laboratory Animals published by China and US National Institutes of Health, adult male Sprague–Dawley (SD) rats (250–300 g) were supplied by the Experimental Animal Center of the Hubei University of Medicine. All animal protocols were approved by the Institutional Animal Care and Use Committee of Hubei University of Medicine.

Model establishment

The left anterior descending coronary artery (LAD) in rats was ligated to prepare the MI model as previously described (Tang et al. 2011). In brief, ketamine (50 mg/kg, i.p.) and xylazine (10 mg/kg, i.p.) were used to anesthetize D rats (250–300 g). LAD ligation was promptly performed after thoracotomy on the left fourth intercostal space after tracheal ventilation remained stable using a Columbus ventilator (HX-300, Taimeng Instruments, Chengdu, China). When confirming the occurrence of myocardial infarction with blanching of the myocardium as well as electrocardiography, the open thoracic cavity was sutured layer by layer immediately.

Vagus nerve stimulation

Surviving rats were randomized into groups with sham or stimulation on the 7th day of myocardial infarction. After the left and right vagal nerves in the neck were gently exposed and separated, the vagal nerve was looped with Teflon-coated stainless-steel wires (UL1330; Triumph Cable Co, Ltd,

China) and linked into the stimulator output part (BL-420 S; Chengdu Tme Technology Co, Ltd, China) for electrical stimulation (20 Hz for 10 s every minute for 4 h) as previously described (Luo et al. 2020). Regular pulse stimulation in the vagal nerve was executed in the vagus nerve stimulation group (VNS) (Luo et al. 2020). Similar operations were performed without initiating stimulation in the sham group (Sham) and MI group (MI). A 10% reduction in heart rate was used as a criterion for VNS. A mixture of white petrolatum (Vaseline) and paraffin was used to immerse the vagus nerve, and electrodes were connected to prevent drying. The inhibition of the inflammatory response after VNS was used as an endpoint criterion, marked by the number of decreased macrophages.

ACh receptor inhibitor treatment in vivo

One hour before VNS, mancamlamine (MLA, 10 mg/kg, ip) or atropine (Atrop, 10 mg/kg, ip) was used to assess whether the role of VNS in SDF-1 α expression in the infarcted heart was linked to mACh-R and α 7-nAChR as described previously (Zhao et al. 2013; Luo et al. 2020). In brief, 7 days after MI, MI rats were randomly divided into four groups, namely, the MI group (MI), MI-VNS group (VNS), MI-VNS-MLA group (VNS + MLA), and MI-VNS-Atrop group (VNS + Atrop). One hour before VNS, the rats in the VNS + MLA and VNS + Atrop groups were injected with MLA (10 mg/kg, ip) or Atrop (10 mg/kg, ip), respectively. Meanwhile, the rats in the MI and VNS groups were injected with an equivalent solvent solution. Finally, the rats in the VNS, VNS + MLA and VNS + Atrop groups were treated by regular pulse stimulation of the vagal nerve. Meanwhile, similar operations were executed in the rats for the Sham and MI groups without initiating stimulation.

Ad-shSDF-1 α preparation and knockdown of SDF-1 α injection in vivo

To determine the effects of VNS on VSMC metabolism and arteriogenesis/angiogenesis in infarcted hearts, an adenovirus carrying SDF-1 α shRNA (Ad-shSDF-1) was used for local injection into the myocardium. Because Ad-shSDF-1 was injected locally into the myocardium, in addition to transfection into the VSMCs of hearts, Ad-shSDF-1 could also be transfected into other cells within the myocardium. In this experiment, the effects of knocking down SDF-1 α could be related to both VSMCs and other cells. Ad-shCtrl and Ad-shSDF-1 were designed using a dedicated program provided by our published data (Tang et al. 2011). Ad-shCtrl and Ad-shSDF-1 α (1×10^9 pfu in 200 μ L) were injected into four sites of the infarcted hearts (50 μ L per site, 12 rats/group) with a 30-gauge tuberculin syringe 3 days before VNS. Two injections were in the myocardium bordering the

ischemic area, and two were within the ischemic area (Tang et al. 2011). Penicillin (150,000 U/mL, i.v.) was given before each procedure. Buprenorphine hydrochloride (0.05 mg/kg, s.c.) was administered twice a day for the first 48 h after the procedure.

Measurement of hemodynamic parameters

Twenty-eight days after treatment, heart functions, including left ventricular systolic pressure (LVSP), left ventricular end-diastolic pressure (LVEDP), and rate of the rise and fall of ventricular pressure ($+dP/dt_{max}$ and $-dP/dt_{max}$), were measured and evaluated using BL-420s (Chengdu Tai-meng, Co, China) as described previously (Tang et al. 2015). Following the anesthesia of rats with the application of ketamine (50 mg/kg, i.p.) and xylazine (10 mg/kg, i.p.), one end of the catheter was connected to a pressure transducer, and the other end of the catheter filled with heparinized (10 U/mL) saline solution was advanced into the left ventricle to record ventricular pressure while it was inserted into the isolated left carotid artery. After evaluating cardiac function, the heart was immediately collected for subsequent detection and analysis.

ELISA for ACh detection

According to the manufacturer's protocol (ab65345, Abcam), ELISA for ACh in heart tissues and blood samples treated with the cholinesterase inhibitor eserine (100 μ M) was performed to confirm these changes in ACh levels in cardiac tissue and serum after VNS.

Immunostaining

Heart tissue serial transverse sections (5 μ m) were prepared as previously described (Tang et al. 2011). Before adding primary antibodies, a blocking buffer (PBS containing 5% goat serum and 0.1% Triton X-100) was used to treat these sections at room temperature for 1 h. The primary antibodies (diluted in blocking buffer), including goat anti-rat SDF-1 α (sc-6193, 1:150; Santa Cruz), mouse anti-rat α -SMA (SC-130,616, 1:150; Santa Cruz), m1-m5-AChR (1:150; Santa Cruz), mouse anti-rat CD31 (ab24590, 1:250; Abcam), CD206 (245,955, 1:200; CST) and rabbit anti-rat CD68 (1:250, GB11067, ServiceBio), were incubated at 4 $^{\circ}$ C overnight, and then the secondary antibodies, including horseradish peroxidase (HRP)-labeled goat anti-mouse IgG, goat-anti-rabbit IgG and rabbit-anti-goat IgG were incubated at room temperature for 2 h (Tang et al. 2011; Cao et al. 2017). Eventually, these indicated results were quantified by densitometry analysis (Image Pro, USA) after taking pictures under a microscope (MF43-N, Olympus, Japan) (Tang et al. 2018). The corresponding negative

controls for the antibodies have been executed, showing no nonspecific binding.

Cell cultures and groups

Human vascular smooth muscle cells (HVSMCs) (Jennio Biotech Co. Ltd, Guangzhou, China) were cultured in complete medium as previously mentioned (Lv et al. 2018). To further assess the mechanisms underlying ACh-induced SDF-1 α expression in HVSMCs, the mACh-R blocker atropine (1 μ M) or nACh-R blocker mecamylamine (7 μ M), PI3K/Akt inhibitor wortmannin (50 nM), eNOS inhibitor L-NAME (300 μ M), MEK/ERK1/2 inhibitor PD98059 (50 μ M), and p38MAPK inhibitor SB203580 (30 μ M) were inoculated for 1 h before treatment with 10^{-5} M ACh for 24 h. For subsequent target molecular detection, these harvested cells were lysed in RAPI buffer containing protease and phosphatase inhibitors (Luo et al. 2020).

Western blot

Western blotting was carried out with primary antibodies against AKT (1:1000, Cell Signaling, #9272s), pAKT (1:1000, Cell Signaling, #9271 s), SDF-1 α (sc-6193, 1:150, Santa Cruz), and α -tubulin (T9026, 1:5000, Sigma). The samples were collected and homogenized on ice in 0.1% Tween-20 homogenization buffer containing protease inhibitors. Fifty micrograms of protein was resolved on a 10% SDS–PAGE gel and transferred onto a polyvinylidene fluoride (PVDF) membrane (Millipore). After being blocked with 5% nonfat milk, the membrane was incubated with primary antibody (1:1000 dilutions) for 90 min followed by incubation with horseradish peroxidase (HRP)-conjugated secondary antibodies (1:10000, Jackson ImmunoResearch). Protein expression was visualized by enhanced chemiluminescence and quantified by densitometry (Tang et al. 2011).

Measurement of vascular density

The numbers of α -SMA or CD31-positive vessels in each section were analyzed in 6–8 equally distributed areas of 0.1 mm² in the peri-infarction or infarction area. The values were then expressed as the number of vessels per squared millimeter. Two independent examiners analyzed these results using the Image-Pro Plus software package (Media Cybernetics, Carlsbad, CA) (Lv et al. 2018; Tang et al. 2011).

Statistical analyses

IBM SPSS statistics software (version 22, 32-bit editing) was used for statistical analysis. <https://www.ibm.com/cn-zh/products/spss-statistics>. The data shown are the mean \pm SD.

Statistical significance between two groups was determined by paired or unpaired Student's *t* test. The results for more than two experimental groups were evaluated by one-way ANOVA to specify differences between groups. $P < 0.05$ was considered significant.

Results

VNS increased CPT1 α expression in VSMCs of the infarcted hearts

To observe the traits of CPT1 α expression in the heart, using immunohistochemical staining, we first found that CPT1 α expression in cardiomyocytes showed higher levels near the blood vessels in normal sham-operated hearts, while its levels were lower in blood vessels (Fig. 1A). After MI, CPT1 α expression was not altered in cardiomyocytes in the peri-infarction area but was obviously decreased in cardiomyocytes in the infarction area (Fig. 1A–C). Then, VNS induced CPT1 α expression in vessels of the peri-infarction and infarction areas in infarcted hearts, especially in VSMCs, in addition to cardiomyocytes (Fig. 1A–C). Last, to confirm the relationship between VNS's effect and cholinergic receptors, we used the mACh-R inhibitor atropine (0.5 mg/kg, ip) or the α 7-nACh-R blocker mecamylamine (1.0 mg/kg, ip) to treat the infarcted heart 1 h after MI and found that the increased CPT1 α expression induced by VNS could be obviously abolished by atropine or mecamylamine, respectively. These results demonstrated that VNS induced CPT1 α expression in the infarcted hearts, especially in the VSMCs of heart vessels, which was related to m/n-ACh-R.

VNS increased CPT1 β expression in VSMCs of the infarcted hearts

To reveal the characteristics of CPT1 β expression in the heart, using immunohistochemical staining, we first found that CPT1 β expression in cardiomyocytes was higher near blood vessels in sham-operated hearts but lower in blood vessels (Fig. 2A–C). After MI, CPT1 β expression was decreased in cardiomyocytes in both the peri-infarction and infarction areas (Fig. 2A). Then, VNS induced CPT1 β expression in vessels of the peri-infarction and infarction areas in infarcted hearts, especially in VSMCs of the infarction area, in addition to cardiomyocytes near the blood vessels (Fig. 2A–C). More importantly, we found that VNS-mediated CPT1 β expression could be obviously abolished by atropine or mecamylamine, indicating that VNS induced CPT1 β expression in the infarcted hearts, especially in the VSMCs of heart vessels.

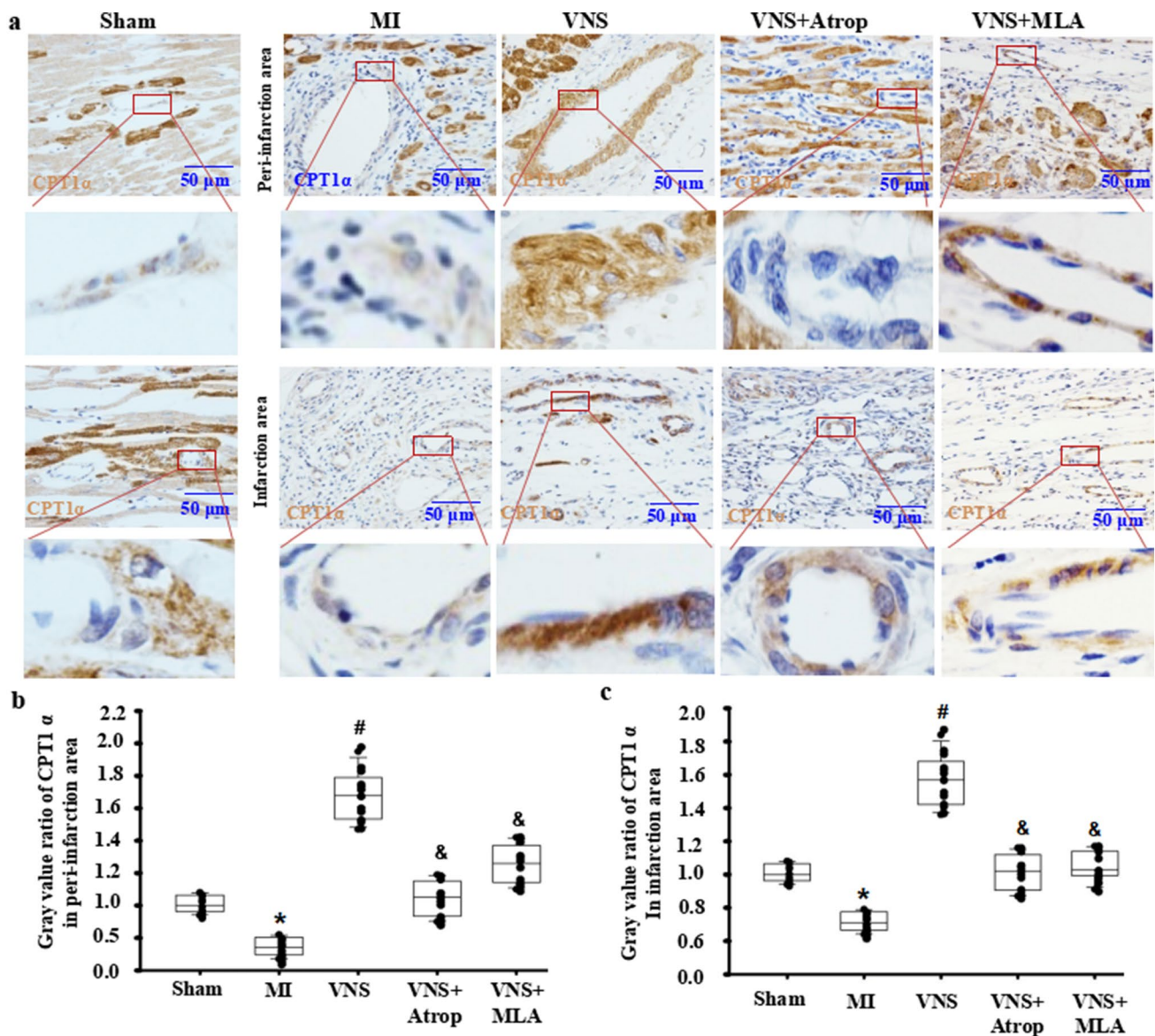


Fig. 1 VNS increased CPT1 α expression in VSMCs in infarcted hearts. **a** Typical immunostaining images for CPT1 α showing that VSMCs were CPT1 α positive, and VNS increased CPT1 α expression in VSMCs of infarcted heart, which could be abolished by atropine (Atrop) or mecamlamine (MLA). Brownish yellow indicates

CPT1 α ; hematoxylin-stained nucleus. **b, c** Semiquantitative analysis of CPT1 α levels in VSMCs of the peri-infarction area (**b**) and infarction area (**c**) of the infarcted hearts. * $P < 0.05$ vs. Sham; # $P < 0.05$ vs. MI; & $P < 0.05$ vs. VNS (n = 12)

VNS slightly increased Glut1 expression in VSMCs of the infarcted hearts

To confirm the traits of Glut1 expression in the heart, using immunohistochemical staining, we first found that Glut1 expression in the vessels of hearts was higher in the sham-operation group, while whether near or far from the blood vessel, its expression levels in cardiomyocytes were low (Fig. 3A). After MI, Glut1 expression was not altered in cardiomyocytes but was slightly increased in vessels of both the peri-infarction and infarction areas, especially in VSMCs (Fig. 3A). Then,

VNS did not markedly change Glut1 in cardiomyocytes but induced Glut1 expression in vessels of the peri-infarction and infarction areas in infarcted hearts, especially in VSMCs (Fig. 3A–C). Meanwhile, we found that VNS-induced Glut1 expression could be obviously abolished by atropine or mecamlamine.

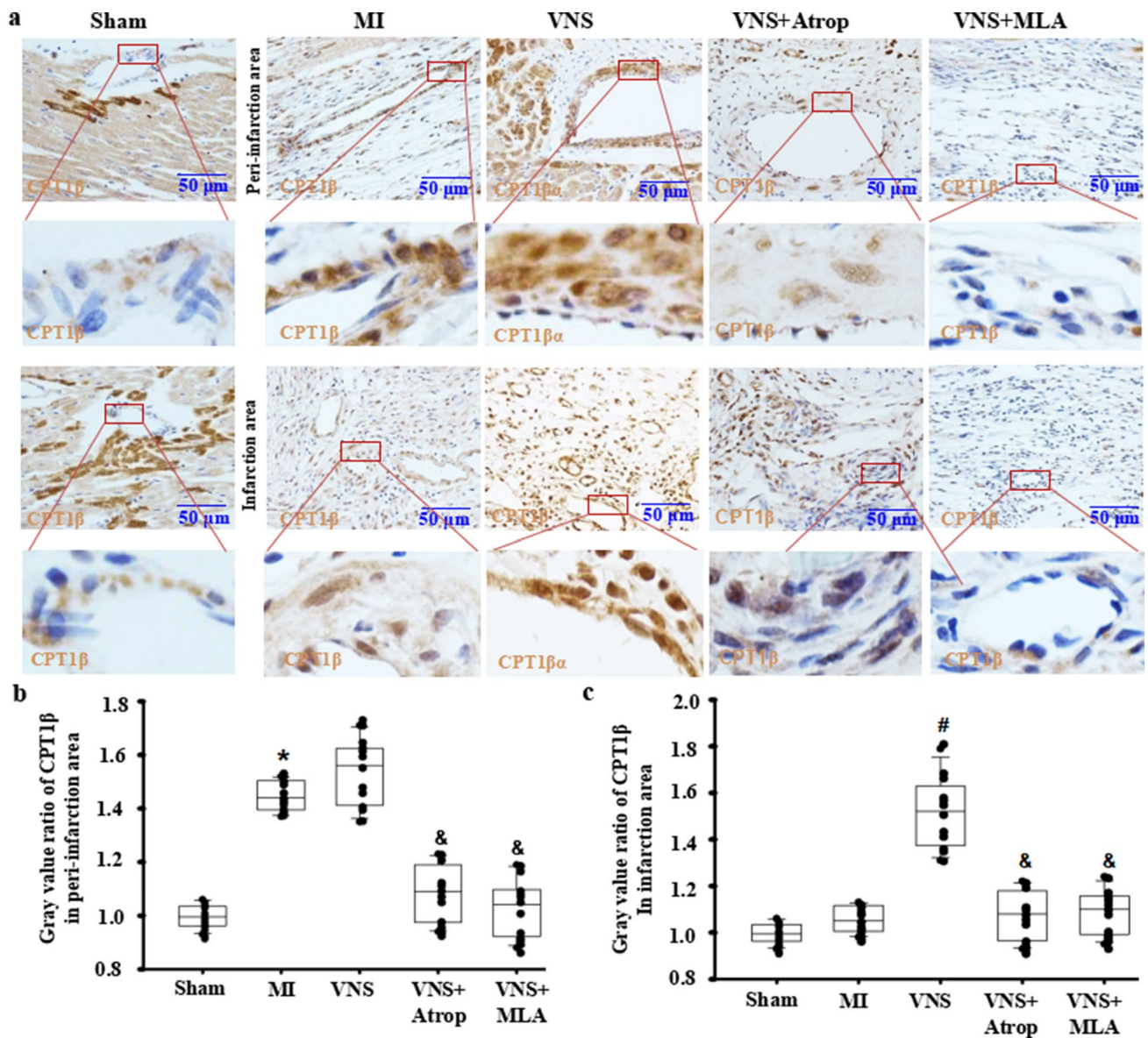


Fig. 2 VNS increased CPT1 β expression in VSMCs of the infarcted hearts. **a** Typical immunostaining images for CPT1 β showing that VSMCs were CPT1 β positive, and VNS increased CPT1 β expression in VSMCs of infarcted heart, which could be abolished by atropine (Atrop) or mecamylamine (MLA). Brownish yellow indicates

CPT1 β ; Hematoxylin-stained nucleus; **b**, **c** Semiquantitative analysis of CPT1 β levels in VSMCs of the peri-infarction area (**b**) and infarction area (**c**) of the infarcted hearts. * $P < 0.05$ vs. Sham; # $P < 0.05$ vs. MI; & $P < 0.05$ vs. VNS ($n = 12$)

VNS slightly changed Glut4 expression in VSMCs of the infarcted hearts

To confirm the traits of Glut4 expression in the heart, using immunohistochemical staining, we first found that Glut4 expression in cardiomyocytes of hearts showed higher levels in the sham-operation group, while its expression levels in vessels were low (Fig. 4A). After MI, Glut4 expression was decreased in cardiomyocytes but increased in vessels in both the peri-infarction and infarction areas, especially in VSMCs (Fig. 4A). Then, VNS markedly increased

Glut4 expression in cardiomyocytes in the peri-infarction area in the infarcted hearts but not in the peri-infarction area of the infarcted hearts. Furthermore, VNS obviously increased Glut4 expression in vessels of the infarction area in infarcted hearts, especially in VSMCs, but not in the peri-infarction of infarcted hearts (Fig. 4A–C). Last, we found that VNS-induced Glut4 expression could be obviously abolished by atropine or mecamylamine, indicating that VNS induced Glut4 expression in both cardiomyocytes and VSMCs of the infarcted hearts through m/n-AChR. These results showed that VNS induced Glut4

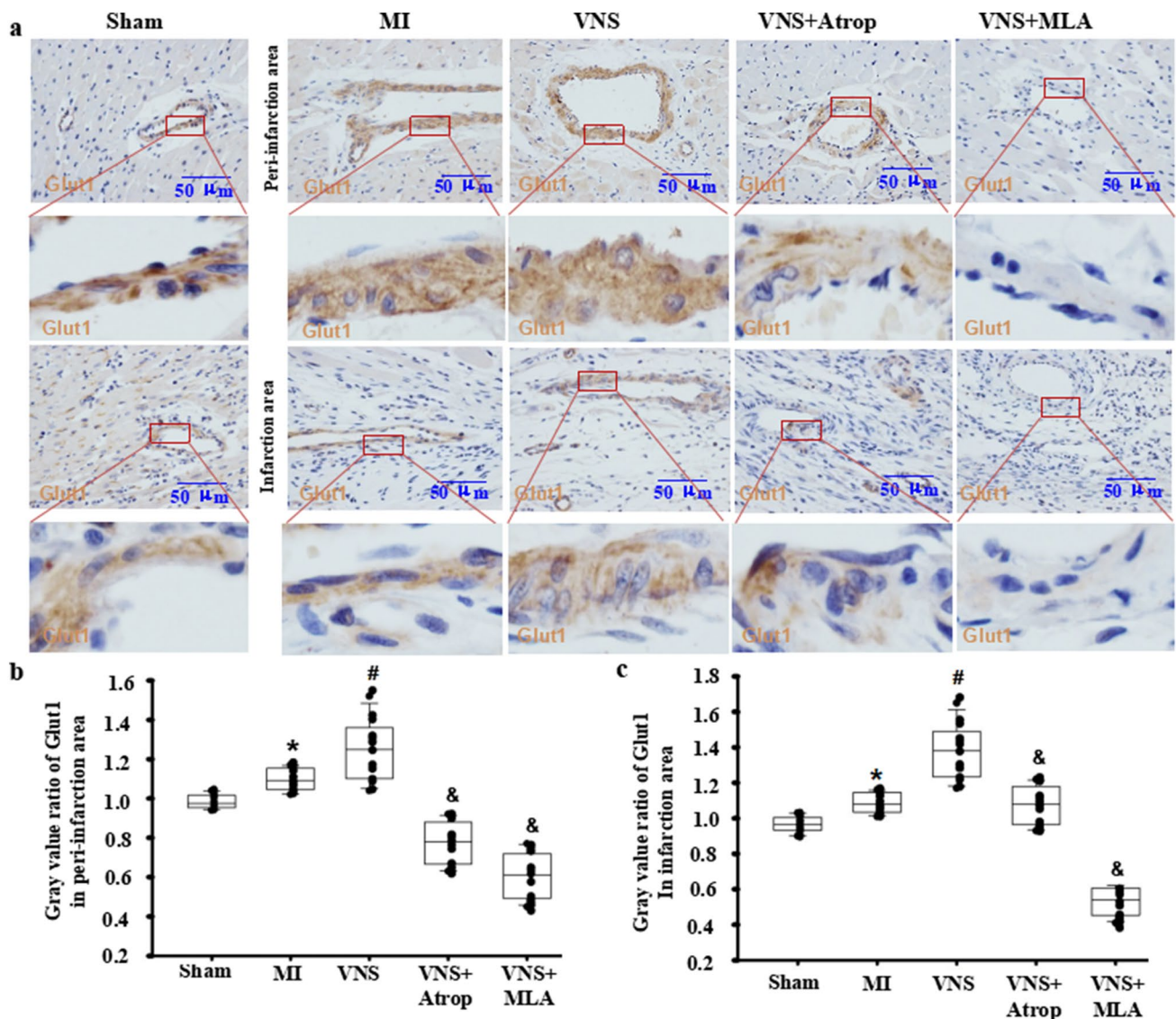


Fig. 3 VNS slightly increased Glut1 expression in VSMCs of the infarcted hearts. **a** Typical immunostaining images for Glut1 showing that VSMCs were CPT1 β positive, and VNS increased Glut1 expression in VSMCs of infarcted heart, which could be abolished by atropine (Atrop) or mecamylamine (MLA). Brownish yellow indicates

Glut1; Hematoxylin-stained nucleus; **b, c** Semiquantitative analysis of Glut1 levels in VSMCs of the peri-infarction area (**b**) and infarction area (**c**) of the infarcted hearts. * $P < 0.05$ vs. Sham; # $P < 0.05$ vs. MI; & $P < 0.05$ vs. VNS ($n = 12$)

expression in the infarcted hearts, especially in VSMCs of heart vessels.

VNS altered M1/M2 macrophages in myocardial infarction through m/n-AChR-SDF-1 α

To confirm whether VNS is involved in macrophages in infarcted hearts, we used immunohistochemical staining for the M1 macrophage marker CD68 and the M2 macrophage marker CD206, as shown in Figs. 5A and E and 6A and E. Compared with the sham group, the numbers of CD68-positive macrophages were increased, while

CD206-positive macrophage cell numbers were decreased, resulting in increased levels of TNF α and IL-1 β (Supplemental Fig. S2) in the infarcted hearts accompanied by an increased ratio of CD68 and CD206 (Figs. 5 and 6). Instead, VNS obviously decreased the number of CD68-positive cells in infarcted hearts. Although CD206 macrophage cell numbers in VNS-treated MI hearts did not obviously increase compared with MI hearts, the ratio of CD68 and CD206 was markedly reduced in the infarcted hearts, leading to decreased levels of TNF α and IL-1 β (Supplemental Fig. S2). Both atropine and mecamylamine abolished the effects of VNS on macrophages and

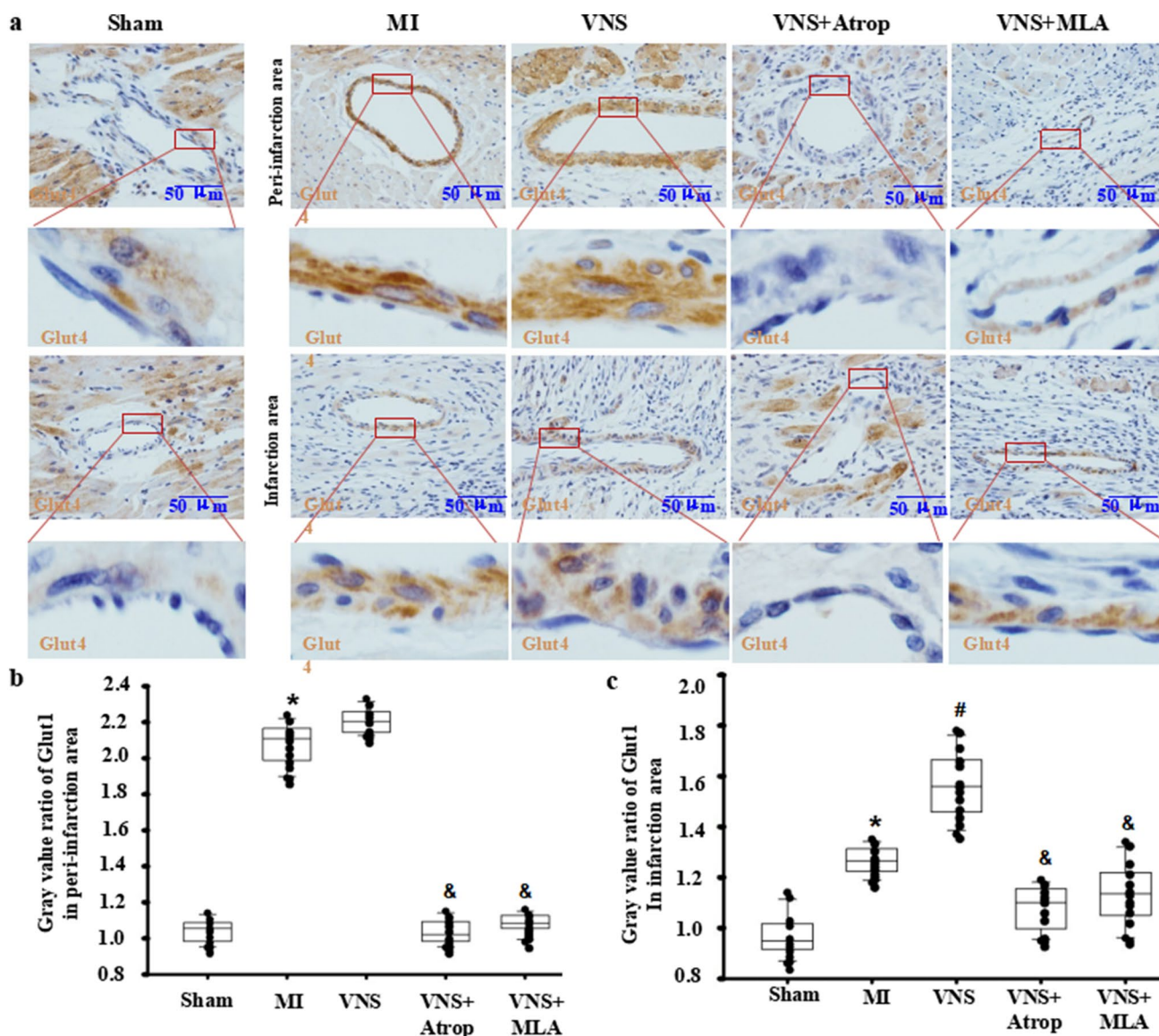


Fig. 4 VNS slightly changed Glut4 expression in VSMCs of the infarcted hearts. **a, b** Typical immunostaining image of Glut4 in the infarction area and peri-infarction area of infarcted hearts treated with mecamylamine (MLA, 10 mg/kg, ip) and atropine (Atrop, 10 mg/kg, ip) before VNS. Brownish yellow indicates Glut4; hematoxy-

lin-stained nucleus. **b, c** Semiquantitative analysis of Glut4 levels in VSMCs in the peri-infarction area (**b**) and infarction area (**c**) of infarcted hearts. * $P < 0.05$ vs. Sham; # $P < 0.05$ vs. MI; & $P < 0.05$ vs. VNS ($n = 12$)

inflammatory factors in infarcted hearts (Figs. 5 and 6). Meanwhile, VNS increased the expression of SDF-1 α in VSMCs of infarcted hearts, and local injection of Ad-shSDF-1 α into the infarcted hearts obviously abolished the induced SDF-1 α expression in infarcted hearts by VNS (Supplemental Fig. S1). Furthermore, knockdown of SDF-1 α in the infarcted hearts obviously abrogated the effect of VNS on macrophages and inflammatory factors in the infarcted hearts (Figs. 5 and 6). These results indicated that VNS altered the ratio of M1/M2 macrophages in myocardial infarction through SDF-1 α .

VNS promoted arteriogenesis and its matching CPT1 α/β and Glut1/4 expression in the infarcted hearts involved in SDF-1 α

To explore whether VNS-induced SDF-1 α is involved in arteriogenesis in infarcted hearts, we used immunohistochemical staining for α -SMA, as shown in Fig. 7A and B. VNS increased the number of α -SMA-positive vessels in infarcted hearts, and the specific effects could be abolished by mAChR or nAChR blockade or SDF-1 α knockdown by shRNA. Then, to confirm whether VNS-induced

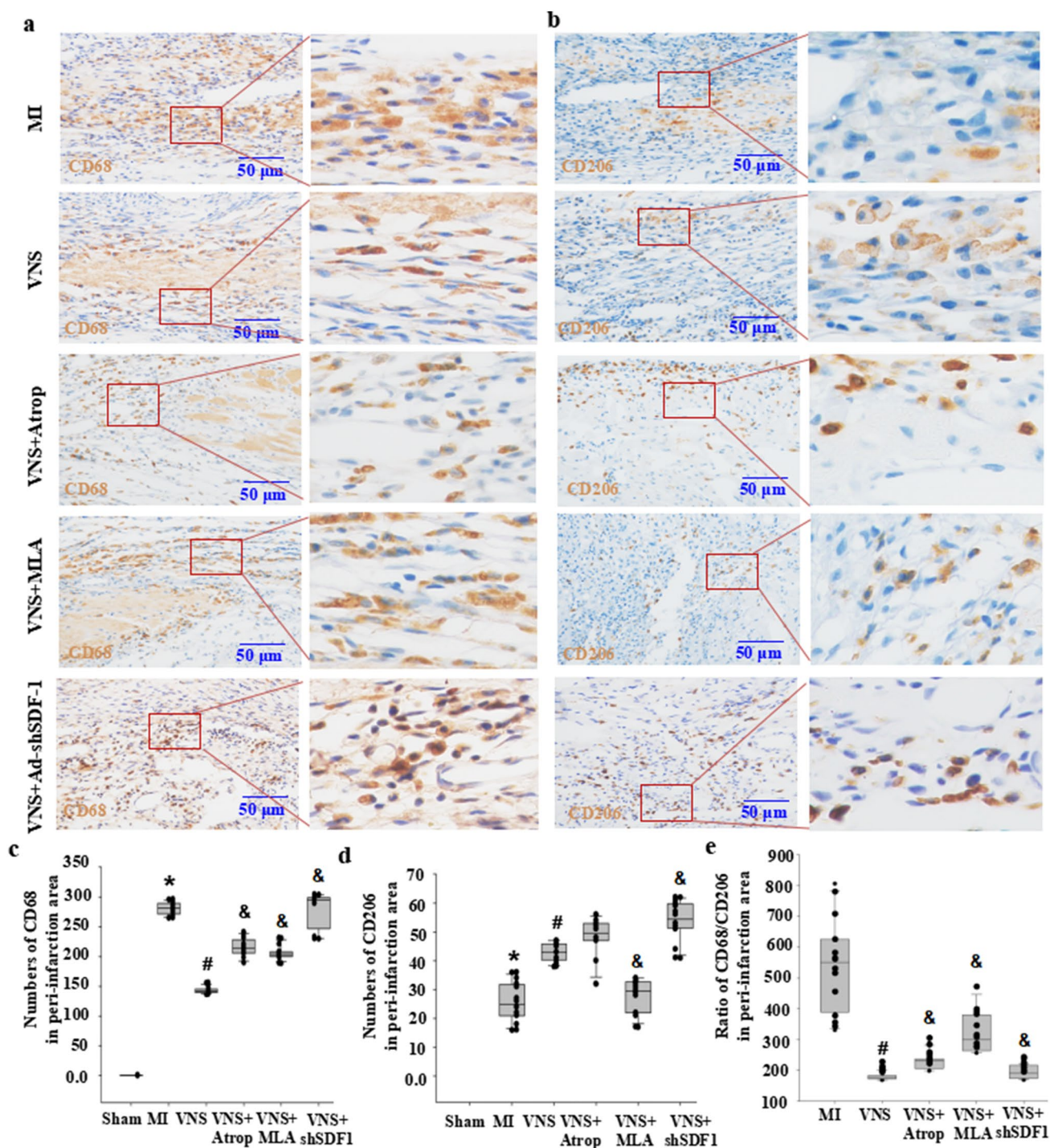


Fig. 5 VNS altered M1/M2 macrophages in the peri-infarction area of myocardial infarction through m/n-AChR-SDF-1 α . **a, b** Typical immunostaining image of CD68 (M1 macrophages) and CD206 (M2 macrophages) in the peri-infarction area of infarcted hearts treated with mancamlamine (MLA, 10 mg/kg, ip), atropine (Atrop, 10 mg/kg, ip) or SDF-1 α knockdown by shRNA (Ad-shSDF-1) before VNS. Brownish yellow indicates CD68 or CD206; hematoxylin-stained

nucleus. **c, d** Semiquantitative analysis of CD68 and CD206 numbers in the peri-infarction area of the infarcted hearts. * $P < 0.05$ vs. Sham; # $P < 0.05$ vs. MI; & $P < 0.05$ vs. VNS ($n = 12$). **e** Semiquantitative analysis of the ratio of CD68/CD206 levels in the peri-infarction area of the infarcted hearts. * $P < 0.05$ vs. Sham; # $P < 0.05$ vs. MI; & $P < 0.05$ vs. VNS ($n = 12$)

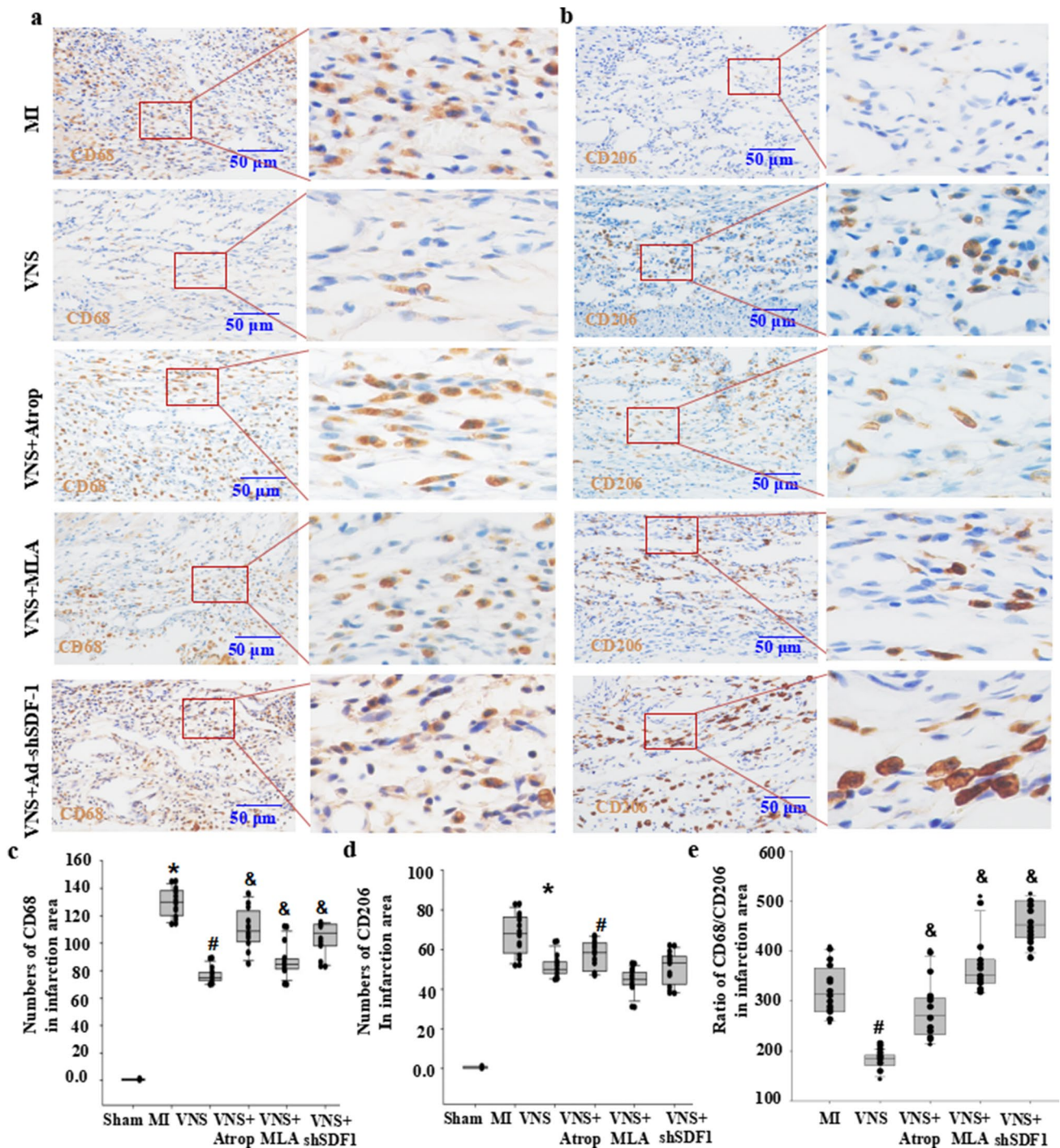


Fig. 6 VNS altered M1/M2 macrophages in the infarction area of myocardial infarction through m/n-AChR-SDF-1 α . **a, b** Typical immunostaining image of CD68 (M1 macrophages) and CD206 (M2 macrophages) in the infarction area of infarcted hearts treated with mancamylamine (MLA, 10 mg/kg, ip), atropine (Atrop, 10 mg/kg, ip) or SDF-1 α knockdown by shRNA (Ad-shSDF-1) before VNS. Brownish yellow indicates CD68 or CD206; hematoxylin-stained

nucleus. **c, d** Semiquantitative analysis of CD68 levels in the infarction area of the infarcted hearts. * $P < 0.05$ vs. Sham; # $P < 0.05$ vs. MI; & $P < 0.05$ vs. VNS ($n = 12$). **e** Semiquantitative analysis of the ratio of CD68/CD206 levels in the infarction area of the infarcted hearts. * $P < 0.05$ vs. Sham; # $P < 0.05$ vs. MI; & $P < 0.05$ vs. VNS ($n = 12$)

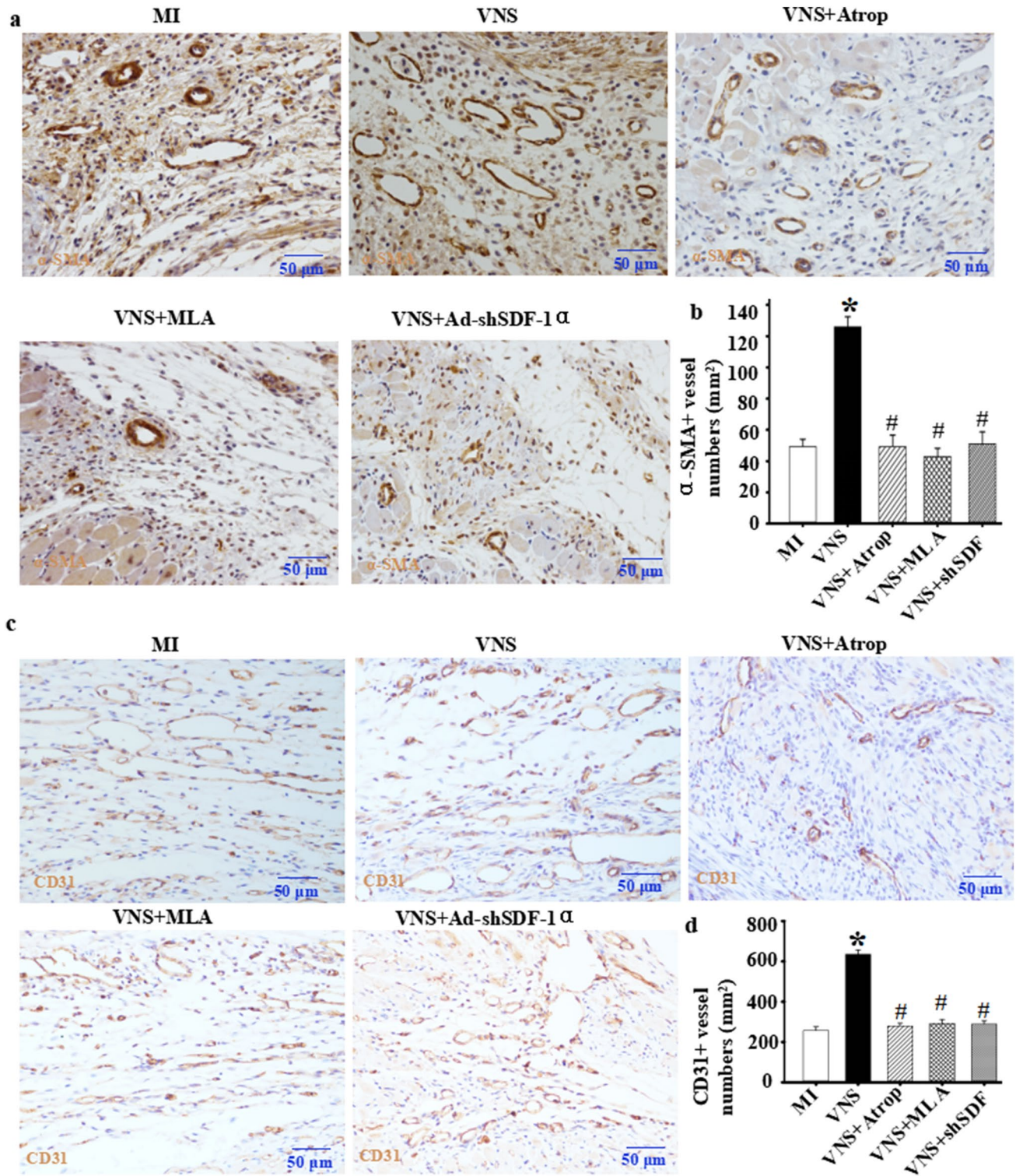


Fig. 7 VNS increased the number of vessels in infarcted hearts. **a** Typical image of α-SMA-positive vessels in infarcted hearts as determined by immunostaining of α-SMA. **b** Quantitative analysis of α-SMA-positive vessels in infarcted hearts. *P<0.05 vs. MI;

P<0.05 vs. VNS. (n=6). **c** Typical image of CD31-positive vessels in infarcted hearts as determined by immunostaining of CD31. **d** Quantitative analysis of CD31-positive vessels in infarcted hearts. *P<0.05 vs. MI; # P<0.05 vs. VNS. (n=6)

SDF-1 α was involved in CPT1 α/β and Glut1/4 expression in the vessels of the infarcted hearts, we used immunohistochemical staining for CPT1 α/β and Glut1/4, and similar to the previous results showing that VNS altered CPT1 α/β and Glut1/4 expression in the infarcted hearts (Figs. 1, 2, 3 and 4), local injection of Ad-shSDF-1 α into the infarcted hearts obviously abolished the induction of CPT1 α/β and Glut1/4 in the infarcted hearts by VNS, indicating that VNS-induced CPT1 α/β and Glut1/4 expression in the infarcted hearts could be related to VNS-induced SDF-1 α expression (Fig. 8).

ACh induced SDF-1 α in VSMCs through the m/n-AChR-Akt signaling pathway

To confirm the relationship between ACh and SDF-1 α mediated by VNS, in vitro VSMCs were treated with different dosages of ACh, as shown in Fig. 9A and B. ACh

induced SDF-1 α expression in a concentration-dependent manner. ACh-induced SDF-1 α was evidently abrogated by atropine and mecamylamine (Fig. 9C and E). Furthermore, ACh-induced SDF-1 α could be dramatically abolished by the PI3K/Akt inhibitor wortmannin (WM) (Fig. 9F and G). These results indicated that ACh could induce SDF-1 α in VSMCs through the m/n-AChR-Akt signaling pathway.

VNS improved cardiac function

Functional analysis was performed to explore whether VNS-induced angiogenesis improved infarcted heart function. The results showed that LV function, including LVSP, LVEDP, + dP/dt_{max}, and - dP/dt_{max}, was significantly improved in VNS-treated hearts compared to MI-treated hearts. SDF-1 α shRNA, however, abolished the VNS-improved LV function (Fig. 10).

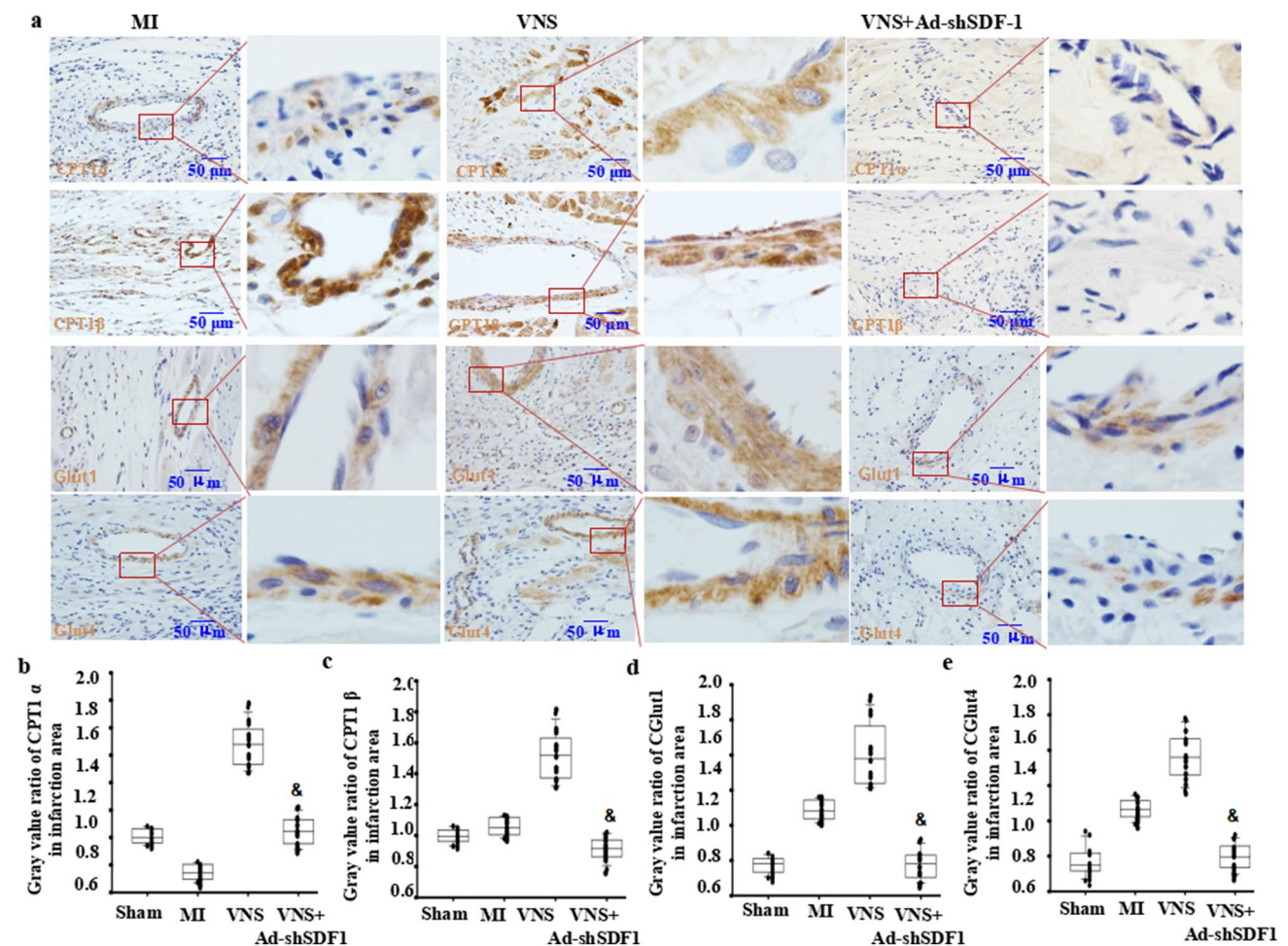


Fig. 8 VNS-mediated CPT1 α/β and Glut1/4 expression in the infarcted heart involves SDF-1 α . **a** Typical immunostaining image of CPT1 α/β and Glut1/4 in the infarction area and peri-infarction area of infarcted heart treated with knockdown of SDF-1 α by shRNA

(Ad-shSDF-1) before VNS. Brownish yellow indicates CPT1 α/β or Glut1/4; hematoxylin-stained nucleus. **b, c** Semiquantitative analysis of CPT1 α/β (**b**) and Glut1/4 (**c**) levels in the infarcted hearts. *P < 0.05 vs. Sham; # P < 0.05 vs. MI; & P < 0.05 vs. VNS (n = 12)

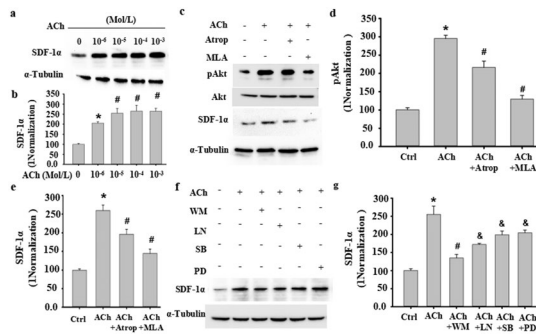


Fig. 9 ACh induced SDF-1 α in VSMCs through the m/n-AChR-Akt signaling pathway. **a, b** ACh dose-dependently induced SDF-1 α expression in VSMCs, as detected by Western blot (**a**). (**b**) Semi-quantitative analysis of SDF-1 α expression in VSMCs. * $P < 0.05$ vs. 0 Mol/L ACh; # $P < 0.05$ vs. 10^{-6} Mol/L ACh ($n = 3$). **c–e** The increased SDF-1 α and phosphorylation of Akt following ACh stimulation in VSMCs was abolished by the mACh-R inhibitor atropine (Atrop) or the nACh-R inhibitor mecamylamine, as determined by Western blot (**c**). **d–e** Semi-quantitative analysis of SDF-1 α expression in VSMCs. * $P < 0.05$ vs. 0 Mol/L ACh; # $P < 0.05$ vs. 10^{-5} Mol/L ACh ($n = 3$). **f–g** Signaling pathways mediating ACh-induced SDF-1 α expression were assessed by pathway-specific inhibitors as indicated. Western blotting was used to detect ACh-induced SDF-1 α expression in VSMCs following treatment with wortmannin (WM, 50 nM), LN (15 nM), SB203580 (SB, 30 μ M), and PD98059 (PD, 50 μ M). α -Tubulin served as an internal control. **g** Semi-quantitative analysis of SDF-1 α in Fig. 7f as indicated. At least three independent experiments were carried out. * $P < 0.05$ vs. 0 ACh (Ctrl); # $P < 0.05$ vs. 10^{-5} Mol/L ACh; # $P < 0.05$ vs. ACh + WM ($n = 3$)

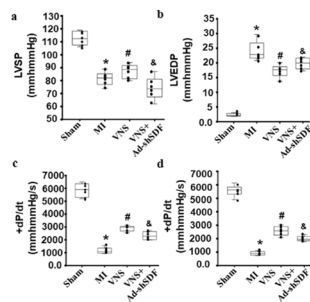


Fig. 10 VNS improved cardiac function. **a–d** Left ventricular systolic pressure (LVSP, **a**), left ventricular end-diastolic pressure (LVEDP, **b**), rate of rise of ventricular pressure (+dP/dt max, **c**), and rate of fall of ventricular pressure (–dP/dt max, **d**) in the VNS group were obviously improved, which could be abolished by Ad-shSDF-1 α . * $P < 0.05$ vs. Sham; # $P < 0.05$ vs. MI; & $P < 0.05$ vs. VNS. ($n = 6$)

Discussion

Preclinical studies demonstrated that VNS could exert protective effects on the heart in animal models of myocardial ischemia–reperfusion, MI and heart failure (Li et al. 2004a; Lim et al. 2016; Martelli et al. 2014; Shen et al. 2011). Multiple mechanisms involved in the

beneficial effects of VNS on the heart. Typically, VNS not only improved parasympathetic tone and reflexes but also inhibited stellate ganglion nerve activity, leading to inhibition of proinflammatory cytokines. Recent findings have shown that VNS can reduce apoptosis and autophagy, suppress oxidative stress and optimize cardiac electrical stability and energy metabolism (Luo et al. 2020). In the present study, VNS increased the greater expression of CPT1 α/β in VSMCs of the infarcted heart than Glut1/4 expression. VNS-induced SDF-1 α expression decreased CD68-positive macrophagecell numbers while increasing CD206-positive macrophagecell numbers, leading to increased α -SMA-positive vessels and functional improvement in infarcted hearts. These results indicated that the protective effects of VNS could be involved in the optimization of VSMC metabolism patterns and arteriogenesis in infarcted hearts.

The cervical vagal nerve contains both afferent and efferent fibers composed of A-, B- and C-fibers (Bonaz et al. 2018). Theoretically, afferent fiber stimulation can be more beneficial for reducing sympathetic activity than efferent fiber stimulation. Regarding the frequency of stimulation, low frequencies (5–10 Hz) activate vagal afferents, whereas high frequencies (10–30 Hz) activate both vagal afferents and efferents (Castoro et al. 2011). Accumulated data have shown that low-level VNS exerts paradoxical effects from high-level VNS (Wang et al. 2019; Johnson et al. 2018). Indeed, in addition to alleviating inflammation, high-level VNS reduced the lower heart rate and inhibited cardiac remodeling (Wu et al. 2023). The reason may be the levels of autonomic imbalance, cardiac inflammation and heart failure, apart from lifestyle factors such as exercise. For example, VNS did not contribute to obvious improvement of heart function in patients with low levels of autonomic imbalance or long-standing heart failure (Sant’Anna et al. 2021). Conversely, VNS was dramatically beneficial for improving heart function in patients with cardiac inflammation (Johnson et al. 2018). In the present study, a frequency of 20 Hz was used, and we found that VNS markedly decreased inflammatory responses in the infarcted heart. These results indicated that the protective effects of VNS could be involved in the inflammatory modulation of the infarcted heart.

Acting as a typical stem cell chemotactic factor, SDF-1 α expression could be controlled by inflammatory cytokines such as IL-1 β and TNF- α . In the infarcted heart, the levels of IL-1 β and TNF- α were obviously increased. VNS significantly reduced their levels in the infarcted heart, leading to increased expression of SDF-1 α , in line with the evidence that IL-1 β promoted SDF-1 α expression, while TNF- α reduced its expression in various cells (Blaine et al. 2011; Krieger et al. 2016; Salvucci et al. 2004). At the same time, it could also align with a recent report that SDF-1 α acted

as an anti-inflammatory chemokine during autoimmune inflammatory responses (Mousavi et al. 2020). In addition, we found that ACh induced SDF-1 α expression in VSMCs under normal culture conditions, which was related to the PI3K/Akt signaling pathway. In summary, these results indicated that VNS at least in part promoted SDF-1 α expression by regulating the inflammatory response.

Previous studies have shown that overexpression of Glut1 in VSMCs promotes chemokine CCL2 and monocyte chemoattractant protein-1 (MCP-1) expression and monocyte recruitment, resulting in excessive inflammatory reactions and accelerating atherosclerosis (Adhikari et al. 2011; Hall et al. 2001; Kaiser et al. 1993; Peiró et al. 2016; Vesely et al. 2009; Wall et al. 2018). Fortunately, we found that VNS did not induce Glut1 expression in the infarcted heart but obviously increased CPT1 α/β expression and anti-inflammatory effects in the infarcted heart, in line with recent reports showing that increased CPT1 α inhibited macrophage influx and the proinflammatory response to delay kidney fibrosis (Yuan et al. 2021). Unfortunately, the present study did not provide detailed information on how VNS regulates the molecular mechanism of CPT1 α/β expression. We only showed superficial results of reduced CPT1 α/β expression after treatment with atropine, mecamylamine or Ad-shSDF, considering the expression of mAChR and $\alpha 7$ -nACh-R in VSMCs (Supplemental Figure S3). However, further in-depth research is needed to determine whether CPT1 α/β , like Glut1, plays a role by regulating SDF-1 α , as well as deeper mechanisms of CPT1 α/β expression mediated by VNS and cholinergic receptors.

Of note, excessive VSMC proliferation and migration could cause atherosclerosis and vessel stenosis, resulting in various vessel-related diseases, including MI (Li et al. 2004b, 2019; Padro et al. 2020; Pestana et al. 2005). Both VSMC proliferation and migration and endothelialization are necessary for arteriogenesis and angiogenesis (Luo et al. 2020; Lv et al. 2018). Previous studies have shown that increased CPT1 α contributes to VSMC proliferation, migration and survival, while excessive glucose metabolism damages VSMCs (Adhikari et al. 2011; Hall et al. 2001; Kaiser et al. 1993; Peiró et al. 2016; Vesely et al. 2009; Wall et al. 2018). In the present study, VNS obviously increased the expression of SDF-1 α and CPT1 α/β in VSMCs in infarcted hearts, leading to more α -SMA-positive vessels, which was consistent with the effects of SDF-1 α and CPT1 α/β on coronary sprouting and lymphangiogenesis (Das et al. 2019; Marín-Juez et al. 2019; Schoors et al. 2015; Wong et al. 2017). These results indicated that the optimized VSMC metabolism pattern induced by VNS could be involved in arteriogenesis and angiogenesis. The detailed mechanism of VNS involving SDF-1 α and CPT1 α/β during the process of arteriogenesis and angiogenesis needs further exploration in the future.

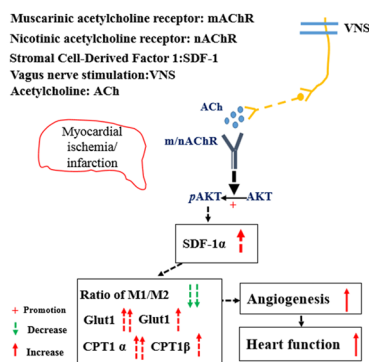


Fig. 11 Working model. VNS improves VSMC metabolism and arteriogenesis in the infarcted heart through m/n-AChR-Akt1-SDF-1 α . VNS and acetylcholine (ACh)-induced SDF-1 α expression optimized the VSMC metabolism pattern characterized by increased CPT1 α/β and Glut1/4 expression while promoting arteriogenesis in the infarcted heart, which was related to the ACh/m/nAChR/Akt signaling cascade

Limitations

Due to the use of male rats in this study, there was no matching experiment with female rats. Previous studies have shown that VNS has more short-term effects in male rats than in female rats (Yaghouby et al. 2020; Yokota et al. 2022). Meanwhile, apart from electrode design and stimulated-side selection, the “dose” of electrical therapies, including current intensity, frequency and duty cycle, could affect the therapeutic effect of VNS on infarcted heart (De Ferrari et al. 2014; Jiao et al. 2016; Kong et al. 2012; Libbus et al. 2017; Nishizaki et al. 2016; Rousselet et al. 2014; Soltani et al. 2023; Wang et al. 2019; Wu et al. 2023; Yu et al. 2016). The present study mainly focused on the effects of VNS on the metabolic patterns of VSMCs and angiogenesis after MI. The different roles of different stimulating parameters in infarcted hearts should be explored in the future.

Taken together, our studies demonstrated that VNS improves heart function by optimizing VSMC metabolism patterns and decreasing inflammatory responses in the infarcted heart via activation of SDF-1 α signaling (Fig. 11).

Supplementary Information The online version contains supplementary material available at <https://doi.org/10.1007/s10735-023-10171-4>.

Acknowledgements Not applicable.

Author contributions XYL and JQL carried out the main animal and cell experiments and drafted the manuscript; YXL and JL had a hand in animal experiments; YW carried out HVSMC cultures; XYL and JQL participated in the immunoassaying; YC and WHH carried out data evaluation; DYK and JMT conceived of the study, participated in the experimental design and coordination of the study, and helped to draft the manuscript. All the authors have read and approved the final manuscript.

Funding This study was supported by grants from the Hubei Provincial Technology Innovation Project (2018ACA162, 2021DFE026 to J.-M.T.), the Foundation of Hubei University of Medicine (HBMUPI201807, FDFR201601 to J.M.T.), Hubei Province's Outstanding Medical Academic Leader Program, the National Natural Science Foundation of China (81670272, 82270299 to J.-M.T.; 31760339 to D.Y.K.); and the Natural Science Foundation of Hubei Province (2020CFB624 to Y.W.).

Data availability Please contact the corresponding author for data requests.

Declarations

Competing interests The authors declare that they have no competing interests.

Ethical approval The study was authorized by the Institutional Review Board of Hubei University of Medicine. Following the Principles of Laboratory Animal Care of China, all rats were kept and used in an SPF grade animal center in accordance with the guidelines.

Consent for publication Not applicable.

Consent to participate The procedures of the balloon injury model in rats were permitted by the Care of Experimental Animals Committee of Hubei University of Medicine.

Open Access This article is licensed under a Creative Commons Attribution 4.0 International License, which permits use, sharing, adaptation, distribution and reproduction in any medium or format, as long as you give appropriate credit to the original author(s) and the source, provide a link to the Creative Commons licence, and indicate if changes were made. The images or other third party material in this article are included in the article's Creative Commons licence, unless indicated otherwise in a credit line to the material. If material is not included in the article's Creative Commons licence and your intended use is not permitted by statutory regulation or exceeds the permitted use, you will need to obtain permission directly from the copyright holder. To view a copy of this licence, visit <http://creativecommons.org/licenses/by/4.0/>.

References

- Adhikari N, Basi DL, Carlson M, Mariash A, Hong Z, Lehman U, Mullegama S, Weir EK, Hall JL (2011) Increase in glut1 in smooth muscle alters vascular contractility and increases inflammation in response to vascular injury. *Arterioscler Thromb Vasc Biol* 31(1):86–94
- Akiyama T, Yamazaki T (2001) Effects of right and left vagal stimulation on left ventricular acetylcholine levels in the cat. *Acta Physiol Scand* 172(1):11–16
- Blaine TA, Cote MA, Proto A, Mulcahey M, Lee FY, Bigliani LU (2011) Interleukin-1 β stimulates stromal-derived factor-1 α expression in human subacromial bursa. *J Orthop Res* 29(11):1695–1699
- Bonaz B, Bazin T, Pellissier S (2018) The vagus nerve at the interface of the microbiota-gut-brain axis. *Front Neurosci* 12:49
- Cao T, Zhang L, Yao L-L, Zheng F, Wang L, Yang J-Y et al (2017) S100B promotes injury-induced vascular remodeling modulating the smooth muscle phenotype. *Biochim Biophys Acta-Mol Basis Dis* 11:2772–2782
- Castoro MA, Yoo PB, Hincapie JG, Hamann JJ, Ruble SB, Wolf PD, Grill WM (2011) Excitation properties of the right cervical vagus nerve in adult dogs. *Exp Neurol* 227(1):62–68
- Ceradini DJ, Kulkarni AR, Callaghan MJ, Tepper OM, Bastidas N, Kleinman ME, Capla JM, Galiano RD, Levine JP, Gurtner GC (2004) Progenitor cell trafficking is regulated by hypoxic gradients through HIF-1 induction of SDF-1. *Nat Med* 10(8):858–864
- Chiong M, Morales P, Torres G, Gutiérrez T, García L, Ibacache M, Michea L (2013) Influence of glucose metabolism on vascular smooth muscle cell proliferation. *Vasa* 42(1):8–16
- Cooke JP, Ghebremariam YT, Coote JH (2008) Endothelial nicotinic acetylcholine receptors and angiogenesis. *Trends Cardiovasc Medicine J Physiol* 18(7):247–253
- Coote JH (2013) Myths and realities of the cardiac vagus. *J Physiol* 591(17):4073–4085
- Das S, Goldstone AB, Wang H, Farry J, D'Amato G, Paulsen MJ, Eskandari A, Hironaka CE, Phansalkar R, Sharma B, Rhee S, Shamskhov EA, Agalliu D, de Perez J, Woo V, Red-Horse YJK (2019) A unique collateral artery development program promotes neonatal heart regeneration. *Cell* 176(5):1128–1142
- De Falco E, Porcelli D, Torella AR, Straino S, Iachininoto MG, Orlandi A et al (2004) SDF-1 involvement in endothelial phenotype and ischemia-induced recruitment of bone marrow progenitor cells. *Blood* 104(12):3472–3482
- De Ferrari GM, Tuinenburg AE, Ruble S, Brugada J, Klein H, Butter C, Wright DJ, Schubert B, Solomon S, Meyer S, Stein K, Ramuzat A, Zannad F (2014) Rationale and study design of the neurocardiac therapy for heart failure study: NECTAR-HF. *Eur J Heart Fail* 16(6):692–699
- Fontana IC, Kumar A, Nordberg A (2023) The role of astrocytic $\alpha 7$ nicotinic acetylcholine receptors in Alzheimer disease. *Nat Rev Neurol* 19(5):278–288
- Greenbaum A, Hsu YM, Day RB, Schuettpeitz LG, Christopher MJ, Borgerding JN, Nagasawa T, Link DC (2013) CXCL12 in early mesenchymal progenitors is needed for hematopoietic stem-cell maintenance. *Nature* 495(7440):227–230
- Hajiasgharzadeh K, Sadigh-Eteghad S, Mansoori B, Mokhtarzadeh A, Shانهbandi D, Doustvandi MA, Asadzadeh Z, Baradaran B (2019) Alpha7 nicotinic acetylcholine receptors in lung inflammation and carcinogenesis: friends or foes? *J Cell Physiol* 234(9):14666–14679
- Hall JL, Chatham JC, Eldar-Finkelman H, Gibbons GH (2001) Upregulation of glucose metabolism during intimal lesion formation is coupled to the inhibition of vascular smooth muscle cell apoptosis: role of GSK3 β . *Diabetes* 50(5):1171–1179
- Jiao J, Harreby KR, Sevcencu C, Jensen W (2016) Optimal vagus nerve stimulation frequency for suppression of spike-and-wave seizures in rats. *Artif Organs* 40(6):E120–E127
- Johnson RL, Wilson CG (2018) A review of vagus nerve stimulation as a therapeutic intervention. *J Inflamm Res* 11:203–213
- Jones CE, Cannon MS (1980) The myocardium and its vasculature: a histochemical comparison of the normal and chronically sympathectomized dog heart. *Histochem J* 12(1):9–22
- Kaiser N, Sasson S, Feener EP, Boukobza-Vardi N, Higashi S, Moller DE, Davidheiser S, Przybylski RJ, King GL (1993) Differential regulation of glucose transport and transporters by glucose in vascular endothelial and smooth muscle cells. *Diabetes* 42(1):80–89
- Kakinuma Y, Ando M, Kuwabara M, Katare RG, Okudela K, Kobayashi M, Sato T (2005) Acetylcholine from vagal stimulation protects cardiomyocytes against ischemia and hypoxia involving additive nonhypoxic induction of HIF-1 α . *FEBS Lett* 579(10):2111–2118
- Kong SS, Liu JJ, Hwang TC, Yu XJ, Zhao M, Zhao M, Yuan BX, Lu Y, Kang YM, Wang B, Zang WJ (2012) Optimizing the

- parameters of vagus nerve stimulation by uniform design in rats with acute myocardial infarction. *PLoS ONE* 7(11):e42799
- Krieger JR, Ogle ME, McFaline-Figueroa J, Segar CE, Temenoff JS, Botchwey EA (2016) Spatially localized recruitment of anti-inflammatory monocytes by SDF-1 α -releasing hydrogels enhances microvascular network remodeling. *Biomaterials* 77:280–290
- Li DJ, Tong J, Zeng FY, Guo M, Li YH, Wang H, Wang P (2019) Nicotinic ACh receptor $\alpha 7$ inhibits PDGF-induced migration of vascular smooth muscle cells by activating mitochondrial deacetylase sirtuin 3. *Br J Pharmacol* 176(22):4388–4401
- Li S, Zhao T, Xin H, Ye LH, Zhang X, Tanaka H, Nakamura A, Kohama K (2004) Nicotinic acetylcholine receptor $\alpha 7$ subunit mediates migration of vascular smooth muscle cells toward nicotine. *J Pharmacol Sci* 94(3):334–338
- Li M, Zheng C, Sato T, Kawada T, Sugimachi M, Sunagawa K (2004) Vagal nerve stimulation markedly improves long-term survival after chronic heart failure in rats. *Circulation* 109(1):120–124
- Libbus I, Nearing BD, Amurthur B, KenKnight BH, Verrier RL (2017) Quantitative evaluation of heartbeat interval time series using poincaré analysis reveals distinct patterns of heart rate dynamics during cycles of vagus nerve stimulation in patients with heart failure. *J Electrocardiol* 50(6):898–903
- Lim GB (2016) Heart failure: vagal nerve stimulation in chronic heart failure. *Nat Rev Cardiol* 13(6):312–312
- Luo B, Wu Y, Liu SL, Li XY, Zhu HR, Zhang L, Zheng F, Liu XY, Guo LY, Wang L, Song HX, Lv YX, Cheng ZS, Chen SY, Wang JN, Tang JM (2020) Vagus nerve stimulation optimized cardiomyocyte phenotype, sarcomere organization and energy metabolism in infarcted heart through FoxO3A-VEGF signaling. *Cell Death Dis* 11(11):971
- Lv YX, Zhong S, Tang H, Luo B, Chen SJ, Chen L, Zheng F, Zhang L, Wang L, Li XY, Yan YW, Pan YM, Jiang M, Zhang YE, Wang L, Yang JY, Guo LY, Chen SY, Wang JN, Tang JM (2018) Vegf-a and vegf-b coordinate the arteriogenesis to repair the infarcted heart with vagus nerve stimulation. *Cell Physiol Biochem* 48(2):433–449
- MacArthur JW Jr, Purcell BP, Shudo Y, Cohen JE, Fairman A, Trubelja A, Patel J, Hsiao P, Yang E, Lloyd K, Hiesinger W, Atluri P, Burdick JA, Woo YJ (2013) Sustained release of engineered stromal cell-derived factor 1- α from injectable hydrogels effectively recruits endothelial progenitor cells and preserves ventricular function after myocardial infarction. *Circulation* 128(11 Suppl 1):S79-86
- Marín-Juez R, El-Sammak H, Helker CSM, Kamezaki A, Mullapuli ST, Bibli SI, Foglia MJ, Fleming I, Poss KD, Stainier Dyr (2019) Coronary revascularization during heart regeneration is regulated by epicardial and endocardial cues and forms a scaffold for cardiomyocyte repopulation. *Dev Cell* 51(4):503-515e4
- Martelli D, McKinley MJ, McAllen RM (2014) The cholinergic anti-inflammatory pathway: a critical review. *Auton Neurosci* 182:65–69
- Mousavi A (2020) CXCL12/CXCR4 signal transduction in diseases and its molecular approaches in targeted-therapy. *Immunol Lett* 217:91–115
- Nishizaki A, Sakamoto K, Saku K, Hosokawa K, Sakamoto T, Oga Y, Akashi T, Murayama Y, Kishi T, Ide T, Sunagawa K (2016) Optimal titration is important to maximize the beneficial effects of vagal nerve stimulation in chronic heart failure. *J Card Fail* 22(8):631–638
- Padro T, Manfrini O, Bugiardini R, Canty J, Cenko E, De Luca G, Duncker DJ, Eringa EC, Koller A, Tousoulis D, Trifunovic D, Vavlukis M, de Wit C, Badimon L (2020) ESC working group on coronary pathophysiology and microcirculation position paper on ‘coronary microvascular dysfunction in cardiovascular disease.’ *Cardiovasc Res* 116(4):741–755
- Peiró C, Romacho T, Azcutia V, Villalobos L, Fernández E, Bolaños JP, Moncada S, Sánchez-Ferrer CF (2016) Inflammation, glucose, and vascular cell damage: the role of the pentose phosphate pathway. *Cardiovasc Diabetol* 15:82
- Pestana IA, Vazquez-Padron RI, Aitouche A, Pham SM (2005) Nicotinic and PDGF-receptor function are essential for nicotine-stimulated mitogenesis in human vascular smooth muscle cells. *J Cell Biochem* 96(5):986–995
- Pillai S, Chellappan S (2012) $\alpha 7$ nicotinic acetylcholine receptor subunit in angiogenesis and epithelial to mesenchymal transition. *Curr Drug Targets* 13(5):671–679
- Rousselet L, Le Rolle V, Ojeda D, Guiraud D, Hagège A, Bel A, Bonnet JL, Mabo P, Carrault G, Hernández AI (2014) Influence of vagus nerve stimulation parameters on chronotropism and inotropism in heart failure. *Annu Int Conf IEEE Eng Med Biol Soc* 2014:526–529
- Salvucci O, Basik M, Yao L, Bianchi R, Tosato G (2004) Evidence for the involvement of SDF-1 and CXCR4 in the disruption of endothelial cell-branching morphogenesis and angiogenesis by TNF- α and IFN- γ . *J Leukoc Biol* 76(1):217–226
- Sant’Anna LB, Couceiro SLM, Ferreira EA, Sant’Anna MB, Cardoso PR, Mesquita ET, Sant’Anna GM, Sant’Anna FM (2021) Vagal neuromodulation in chronic heart failure with reduced ejection fraction: a systematic review and meta-analysis. *Front Cardiovasc Med* 8:766676
- Schoors S, Bruning U, Missiaen R, Queiroz KC, Borgers G, Elia I, Zecchin A, Cantelmo AR, Christen S, Goveia J, Heggermont W, Goddè L, Vinckier S, Van Veldhoven PP, Eelen G, Schoonjans L, Gerhardt H, Dewerchin M, Baes M, De Bock K, Ghesquière B, Lunt SY, Fendt SM, Carmeliet P (2015) Fatty acid carbon is essential for dNTP synthesis in endothelial cells. *Nature* 520(7546):192–197
- Shen MJ, Shinohara T, Park HW, Frick K, Ice DS, Choi EK, Han S, Maruyama M, Sharma R, Shen C, Fishbein MC, Chen LS, Lopshire JC, Zipes DP, Lin SF, Chen PS (2011) Continuous low-level vagus nerve stimulation reduces stellate ganglion nerve activity and paroxysmal atrial tachyarrhythmias in ambulatory canines. *Circulation* 123(20):2204–2212
- Soltani D, Azizi B, Sima S, Tavakoli K, Hosseini Mohammadi NS, Vahabie AH, Akbarzadeh-Sherbaf K, Vashghani-Farahani A (2023) A systematic review of the effects of transcutaneous auricular vagus nerve stimulation on baroreflex sensitivity and heart rate variability in healthy subjects. *Clin Auton Res* 33(2):165–189
- Tang JM, Luo B, Xiao JH, Lv YX, Li XL, Zhao JH, Zheng F, Zhang L, Chen L, Yang JY, Guo LY, Wang L, Yan YW, Pan YM, Wang JN, Li DS, Wan Y, Chen SY (2015) VEGF-A promotes cardiac stem cell engraftment and myocardial repair in the infarcted heart. *Int J Cardiol* 183:221–231
- Tang JM, Shi N, Dong K, Brown SA, Coleman AE, Boegehold MA, Chen SY (2018) Response gene to complement 32 maintains blood pressure homeostasis by regulating α -adrenergic receptor expression. *Circ Res* 123(9):1080–1090
- Tang JM, Wang JN, Zhang L, Zheng F, Yang JY, Kong X, Guo LY, Chen L, Huang YZ, Wan Y, Chen SY (2011) VEGF/SDF-1 promotes cardiac stem cell mobilization and myocardial repair in the infarcted heart. *Cardiovasc Res* 91(3):402–411
- Vesely ED, Heilig CW, Brosius FC 3 (2009) GLUT1-induced cFLIP expression promotes proliferation and prevents apoptosis in vascular smooth muscle cells. *Am J Physiol Cell Physiol* 297(3):C759–C765
- Wall VZ, Barnhart S, Kanter JE, Kramer F, Shimizu-Albergine M, Adhikari N, Wight TN, Hall JL, Bornfeldt KE (2018) Smooth muscle glucose metabolism promotes monocyte recruitment and

- atherosclerosis in a mouse model of metabolic syndrome. *JCI Insight* 3(11):e96544
- Wang Y, Po SS, Scherlag BJ, Yu L, Jiang H (2019) The role of low-level vagus nerve stimulation in cardiac therapy. *Expert Rev Med Devices* 16(8):675–682
- Wong BW, Wang X, Zecchin A, Thienpont B, Cornelissen I, Kalucka J, García-Caballero M, Missiaen R, Huang H, Brüning U, Blacher S, Vinckier S, Goveia J, Knobloch M, Zhao H, Dierkes C, Shi C, Hägerling R, Moral-Dardé V, Wyns S, Lippens M, Jessberger S, Fendt SM, Luttun A, Noel A, Kiefer F, Ghesquière B, Moons L, Schoonjans L, Dewerchin M, Eelen G, Lambrechts D, Carmeliet P (2017) The role of fatty acid β -oxidation in lymphangiogenesis. *Nature* 542(7639):49–54
- Wu Z, Liao J, Liu Q, Zhou S, Chen M (2023) Chronic vagus nerve stimulation in patients with heart failure: challenge or failed translation? *Front Cardiovasc Med* 10:1052471
- Yaghoubi F, Jang K, Hoang U, Asgari S, Vasudevan S (2020) Sex differences in vagus nerve stimulation effects on rat cardiovascular and immune systems. *Front Neurosci* 14:560668
- Yokota H, Edama M, Hirabayashi R, Sekine C, Otsuru N, Saito K, Kojima S, Miyaguchi S, Onishi H (2022) Effects of stimulus frequency, intensity, and sex on the autonomic response to transcutaneous vagus nerve stimulation. *Brain Sci* 12(8):1038
- Yu JG, Song SW, Shu H, Fan SJ, Liu AJ, Liu C, Guo W, Guo JM, Miao CY, Su DF (2013) Baroreflex deficiency hampers angiogenesis after myocardial infarction via acetylcholine- α 7-nicotinic ACh receptor in rats. *Eur Heart J* 34(30):2412–2420
- Yu L, Wang S, Zhou X, Wang Z, Huang B, Liao K, Saren G, Chen M, Po SS, Jiang H (2016) Chronic intermittent low-level stimulation of tragus reduces cardiac autonomic remodeling and ventricular arrhythmia inducibility in a post-infarction canine model. *JACC Clin Electrophysiol* 2(3):330–339
- Yuan Q, Lv Y, Ding H, Ke Q, Shi C, Luo J, Jiang L, Yang J, Zhou Y (2021) CPT1 α maintains phenotype of tubules via mitochondrial respiration during kidney injury and repair. *Cell Death Dis* 12(8):792
- Zhao M, He X, Bi XY, Yu XJ, Gil Wier W, Zang WJ (2013) Vagal stimulation triggers peripheral vascular protection through the cholinergic anti-inflammatory pathway in a rat model of myocardial ischemia/reperfusion. *Basic Res Cardiol* 108(3):345

Publisher's Note Springer Nature remains neutral with regard to jurisdictional claims in published maps and institutional affiliations.